iScience

Article

The liquid-vapor water generation characteristics of thermo-responsive polymer based on the multi-scale method

Graphical abstract

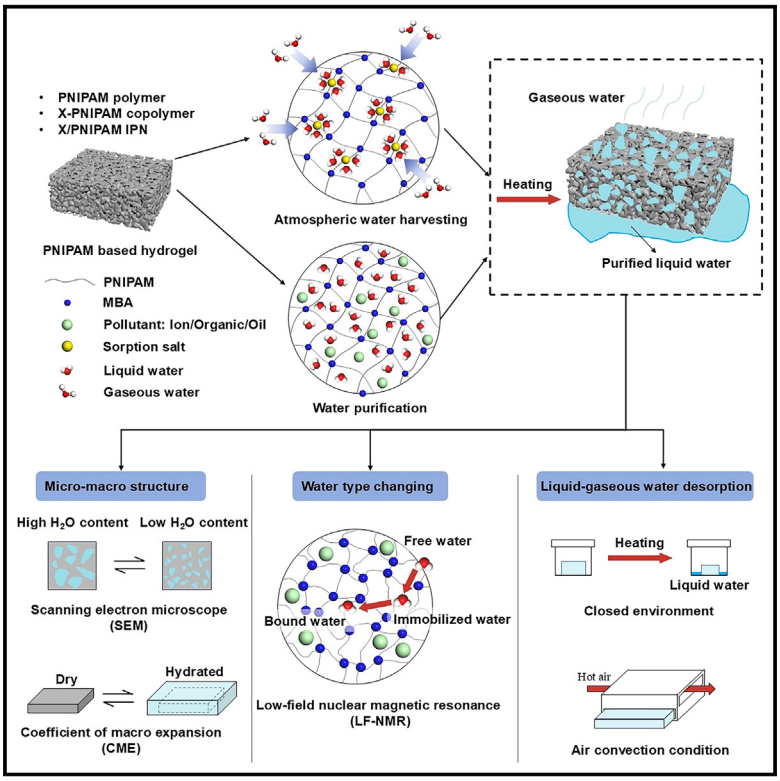

Highlights

- Micro-macro method used for the structure and desorption of a thermo-responsive polymer
- Free and immobilized water become immobilized and bound water during desorption
- Liquid water desorption ratio is 80% and 21% in close and air convection condition
- 15.4 g $kg^{-1} \cdot min^{-1}$ liquid water can be collected directly in a closed environment

Authors

Shaochen Tian (田少宸), Chaoyang Chen (陈超洋), Lei Huang (黄磊), Xueliang Yao (姚雪亮), Anming She (佘安明), Xing Su (苏醒)

Correspondence

suxing@tongji.edu.cn

In brief

Macromolecules; Materials science; Polymers

Tian et al., 2025, iScience *28*, 111619
January 17, 2025
https://doi.org/10.1016/j.isci.2024.111619

CellPress

iScience

CellPress
OPEN ACCESS

Article

The liquid-vapor water generation characteristics of thermo-responsive polymer based on the multi-scale method

Shaochen Tian (田少宸),[1] Chaoyang Chen (陈超洋),[1] Lei Huang (黄磊),[2] Xueliang Yao (姚雪亮),[3] Anming She (佘安明),[3] and Xing Su (苏醒)[1,4,*]

[1]School of Mechanical Engineering, Tongji University, Shanghai 201804, China
[2]Jiangsu JINYOU New Material Co., Ltd., Nantong, Jiangsu 226151, China
[3]School of Materials Science and Engineering, Tongji University, Shanghai 201804, China
[4]Lead contact
*Correspondence: suxing@tongji.edu.cn
https://doi.org/10.1016/j.isci.2024.111619

SUMMARY

Thermo-responsive polymer is becoming a potential water purification and water harvesting material. To clarify the water diffusion characteristics, the desorption ratio of liquid water and water vapor for a poly (N-isopropylacrylamide) was researched by the multi-scale method. Firstly, macro and micro structures for the hydrogel with different water content were characterized. Second, the dynamic moisture preserving status of the hydrogel during the desorption process were tested. Thirdly, the dynamic liquid-vapor desorption rate was quantified. The macro volume of the polymer is of liner relationship with water content. During the desorption process, free and immobilized water transfers to immobilized and bound water. About 80% of the purified liquid water can be collected directly in closed environment, while the amount decreased to 21%–25% in air convection condition. The results suggested a heating method for improving liquid water collection rate with low energy cost for practical applications.

INTRODUCTION

Energy and water resources have always been severe topics. Only 2.5% of Earth's water is fresh water, and the amount of fresh water still declines due to contamination.[1,2] Among the water production and water purification technologies, atmospheric adsorption-based water purification and water harvesting have been proven to be a potential method for providing fresh water.[3–5] Thermo-responsive polymers (TRP) have special behavior around the lower critical solution temperature (LCST).[6,7] When the ambient temperature is lower than the LCST, TRPs can adsorb the solution and become swollen. When heated to a temperature higher than the LCST, TRPs will shrink and release the adsorbed components.[8] Typical TRPs are based on poly(N-isopropylacrylamide) (PNIPAM), poly(N-vinyl caprolactam) (PVCL), poly (vinyl methyl ether) (PVME), poly(oligo (ethylene glycol) methacrylate) (POEGMA) and et al. Many of the PNIPAM based TRPs have the LCST around 32°C,[9,10] and the LCST of PVCL, PVME, and POEGMA are 30∼50°C,[11] 37°C[12] and 27–60°C,[13] respectively. This kind of polymer has a wide range of applications, in terms of controlled drug delivery,[14,15] thermal management of high-safety electrochemical storage devices[16] and buildings,[17] dehumidification,[18] humidity sensor[19] and et al. Affected by the neurotoxicity of PNIPAM, PVCL[20] and POEGMA[21] based TRPs, with high biocompatibility, are more suitable for the application of biological field than PNIPAM. Thermo-responsive block copolymers, interpenetrating network TRPs have higher performance in specific aspect than copolymers. The swelling performance of TRPs can be improved by forming copolymers with polyethylene glycol (PEG),[22] and high hydrophilicity and equilibrium swelling rate can be achieved by combining with sodium acrylate (SA).[23] Applying crosslinker, e.g., N,N,N′,N′-tetramethylenediamine,[24] or forming double network with electrostatic co-monomer, 2-acrylamido-2-methylpropane sulfonic acid (AMPS)[25] can obtain TRPs with high mechanical property. In recent years, TRPs have been widely researched in water production applications, including atmospheric water harvesting[10] and waste water purification treatment.[26,27]

For atmospheric water harvesting, the water vapor adsorption rate for gel by crosslinking PNIPAM with N, N′-methylenebisacrylamide is 0.3 g/g.[28] The mount of hygroscopic salt, e.g., LiCl and $CaCl_2$, can increase the water absorption capacity of TRPs to 1.7 g/g,[17,29] and liquid water can be obtained by heating the temperature to higher than the LCST. The crosslinking with photothermal material, the liquid water desorption process can be driven by the solar, achieving high energy efficiency.[30] By combining TRPs with solution and energy devices, water generation can be achieved with the coefficient of performance rising to more than 4 times at most.[31] These kinds of TRPs are developed on the principle of water vapor capturing performance improvement and water production with low energy consumption.

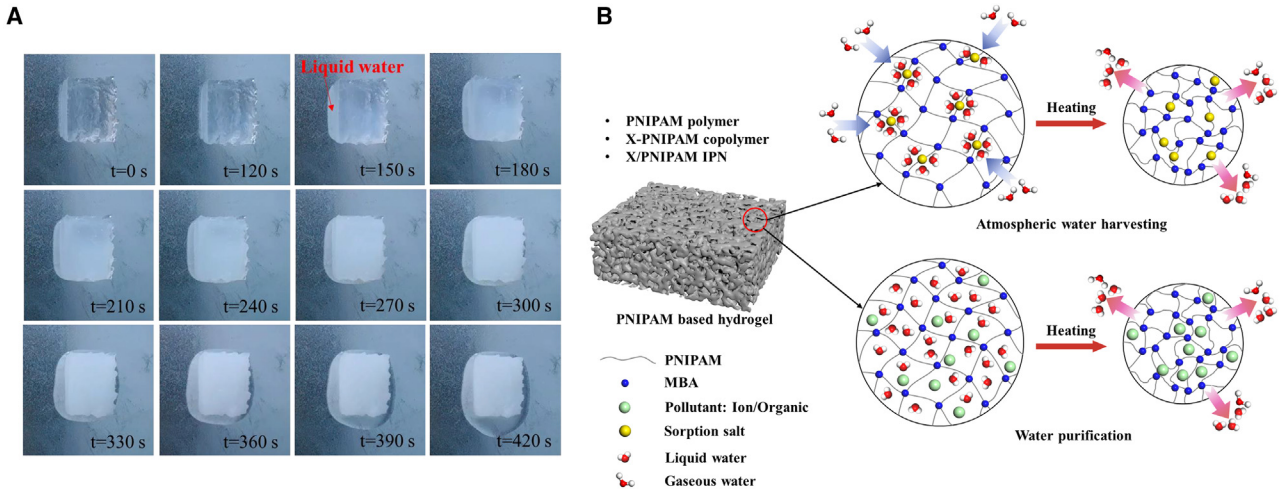

Figure 1. Liquid water desorption and application of PNIPAM hydrogel

(A) Liquid water desorption process by heating PNIPAM hydrogel.

(B) Schematic figure of the water purification and water harvesting of PNIPAM based hydrogel.

When it comes to the application for wastewater purification, ions,[32] oil and salt (desalination)[33] can be removed by TRPs. TRPs based forward osmosis have been widely researched for the purification of salt ions.[34–36] The low temperature gel can adsorb water from wastewater through forward osmosis, and generates purified water when heated to above the LCST. Similar to the reversible hydrophilic-hydrophobic transitions on metal surfaces,[37] the separation of water and oil for TRPs is based on the transition from hydrophilic-oleophobic under low temperature to the hydrophobic-oleophilic heating to above the LCST,[26] about 45°C.[38] In convers, based on the hydrophilicity and underwater superoleophobicity under low temperature, the dissolved water in oil can also be adsorbed under the LCST. As for the removing of ions or organic dyes in polluted water, sorption properties and thermo-responsive properties can achieve pollutant sorption and purified water release when heated to above the LCST, respectively.[39] Ni ion (70%),[40] Cu^{2+},[41] and Hg(II) ions[42] can be removed by the corresponding adsorption segment of PNIPAM based thermal-responsive polymer. For removing the organic pollutants in the wastewater, the adsorption composites are different.[43–46] However, the above researches are of the mixing and flocculation method, and the heating of the whole system to 60°C[47] is required. To reduce the heating energy, dried block TRPs can be put into the polluted water to achieve the absorption of water and pollutant.[48] After the adsorption process under low temperature, more than 20 g/g,[30] the purified water and the pollutant in TRP gels can be separated.[49] After heating the swollen TRPs block to above the LCST, the chemical deposited pollutant can be maintained in the gel, and liquid water is desorbed.[50] Thus, the block TRP materials will be an energy efficient water purification method.

It can be generalized that for atmospheric water harvesting and water purification regeneration process of TRP materials, the heating to shrink water release is a necessary process. During the desorption process, both macro and micro structure variate with the adsorption water amount.[51] The porous parameters of PNIPAM based hydrogel for removing the pollutant are the crucial factors for mass transport, and the diameter can be controlled by temperature induced swollen and shrinking.[52] Scanning electron microscopy (SEM) and nuclear magnetic resonance (NMR) are effective methods for characterizing the microstructure, as well as revealing the hydration mechanism of porous materials.[53] The pore structure and surface morphology of a TRP membrane can be characterized by using field emission SEM.[54] However, the dynamic porous parameters were not involved, especially for water uptake related porous parameters. On the other hand, for the thermal driven desorption process of TRPs block, gaseous water is also available.[55] By condensing the water vapor, about 1.31 g $g^{-1}\cdot day^{-1}$ water can be generated of a PNIPAM based core-shell hydrogel.[56] In general, the revealing of liquid-gaseous desorption characteristic is highly recommended for high efficiency purified water generation.

In brief, the existing research is mainly concentrated on developing high performance TRP hydrogels, neglecting the characterization during the desorption processes, as well as the vapor-liquid two-phase desorption performance. To address this research gap for further understanding the liquid water desorption mechanism and to provide a desorption strategy for different applications, this research combines micro desorption characterization experiment and macro desorption test experiment toward a PNIPAM hydrogel (typical TRP with LCST of 32°C). Firstly, the macro and micro structures for the hydrogel with different water content were characterized by macro volume measurement methods and SEM. Second, by using low-field nuclear magnetic resonance (LF-NMR), the dynamic moisture preserving conditions of the hydrogel during the desorption process were tested. Thirdly, two experimental setups were built for testing the liquid water and water vapor desorption ratio, under a closed environment and air convection environment, from a macro perspective. The dynamic liquid-vapor desorption rate was quantified separately.

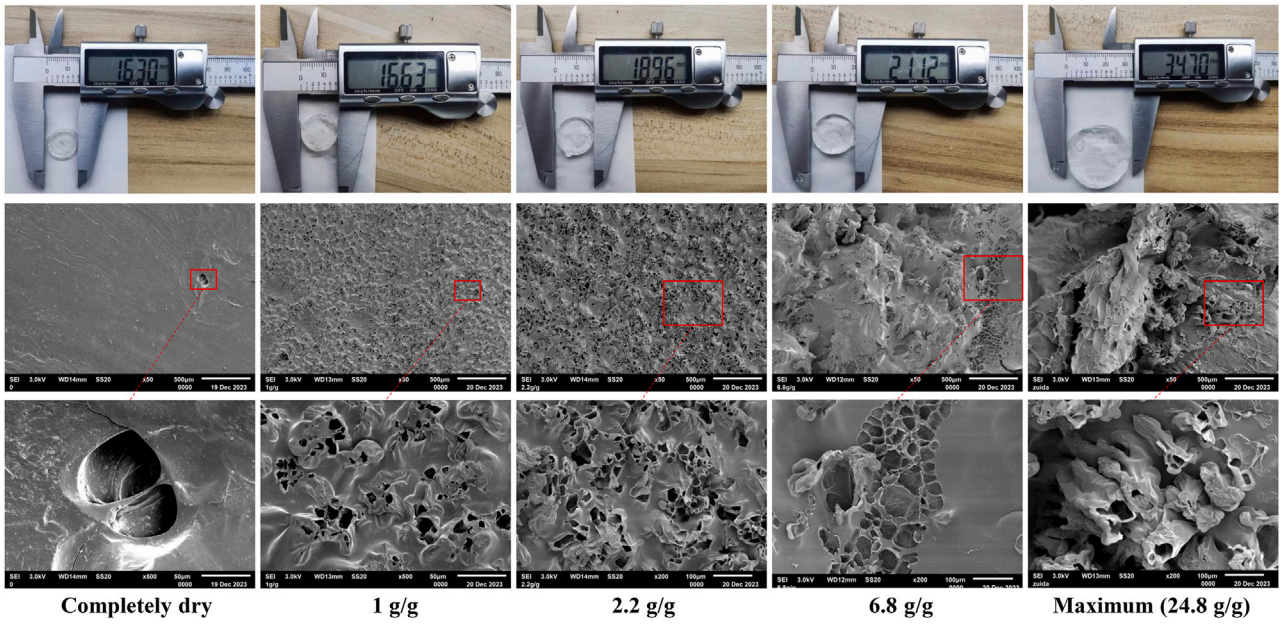

Figure 2. Macro structure and SEM images of PNIPAM hydrogel under different water content

Both macro volume and micro pore diameter increases with the rising of water content; scale bar, 500 μm for all middle line images, 50 μm for bottom line images with water content of completely dry and 1 g/g, 100 μm for bottom line images with water content of 2.2 g/g, 6.8 g/g and maximum.

RESULTS

Bulk volume and porous parameter decrease during desorption

The prepared PNIPAM hydrogel was placed on a heating plate to observe the liquid water desorption process. The heating temperature of the plate was set at 80°C. The desorption process and the schematic figure of the water purification and water harvesting of the PNIPAM based hydrogel are shown in (Figures 1A and 1B).

The PNIPAM hydrogel transferred from transparent to opaque, after being heated to a temperature higher than the LCST. After the PNIPAM becomes opaque, the discharge of liquid water can be observed. The change in transparency and water desorption process takes only several minutes. Based on the process, the shrinkage induced water release can generate liquid water directly, from both atmosphere and pollutant water, by using PNIPAM based polymer hydrogels.

The macro and micro surface structure of the PNIPAM hydrogel, of under different water content, testing results are shown in (Figure 2). It can be found that both the pore diameter of microstructure and macro size have a significant correlation with water content.

The surface of the PNIPAM hydrogel is smooth when the water content is 0 g/g (completely dry). There is almost no pore except for very few porous structures of large volume. The large volume of pore structure may be attributed to the small amount of the residual water after the drying process. With the water content increases to the maximum adsorption amount, the pore diameter increases, and the micro surface gets rough. The macro structure of the PNIPAM hydrogel is also affected by the adsorbed water amount and gel fraction. With the water content varies from 0 g/g to the maximum value, the diameter of the gel increases to 34.30 mm from 16.30 mm, accordingly.

To accurately quantify the macro structure under different water content, bulk volumes of the gel are tested further. To reduce the deviation caused by the synthesis process, two samples based on the same synthesis process were tested by using the same method. The testing results and the CME calculation results of the PNIPAM hydrogel are shown in (Figures 3A and 3B).

For both two PNIPAM samples, the bulk volume is of linear relationship with the variation of water content, and the goodness of fit is higher than 0.999 for both samples. The gel fraction of PNIPAM hydrogel reduces with the rising of water content. For completely dried PNIPAM gel, the gel fraction reaches 100%. When the water content increases to 11.411 g, the gel fraction reduced to 9.37% for sample-1. For sample 2, the gel fraction is 8.66%, with a water content of 11.134 g. Thus, with a high water content of PNIPAM hydrogel, the adsorbed water takes more than 90% of the weight, representing the high water adsorption capacity of such gel.

The calculated CME ranges from 0.73 to 0.99 m^3/kg. It should be noted that the lowest CME values are found at a low water content of 0.234 g/g and 0.288 g/g for sample-1 and sample-2, respectively. The corresponding CME are both 0.73 m^3/kg. Due to the large deviations under low water content, the 0.73 m^3/kg was not included into consideration. The calculated average CME is 0.94 m^3/kg, by considering both two samples. During the desorption process, both the solid volume and mass of the PNIPAM skeleton do not change. Thus, the loss of the water will result in a reduction of the porosity of the PNIPAM skeleton, and the reduction rate equals to the CME.

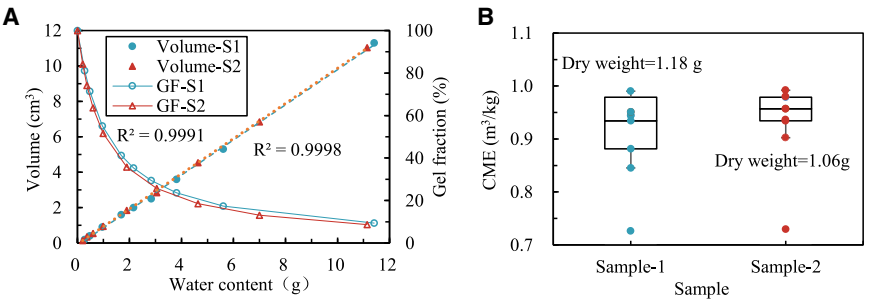

Figure 3. Macro volume and weight characteristics of PNIPAM hydrogel

Sample-1 (S1) and sample-2 (S2) has similar bulk volume, gel fraction and CME parameters.

(A) Volume and gel fraction under different water weight. Data are represented as the result of single experiment of each sample.

(B) CME calculation results. Data are represented as the box-plot of each sample.

Amorphous structure of poly(N-isopropylacrylamide)

The XRD spectra for the PNIPAM sample are shown in Figure S4. It shows a broad diffraction peak at around $2\theta = 20.84°$, indicating the amorphous structure of the PNIPAM. The results have similar variation trends with the PNIPAM hydrogel XRD results in ref. [57].

Special thermal properties

The differential scanning calorimetry (DSC) and thermal diffusion coefficient (TDC) testing results of the completely dried PNIPAM are shown in (Figures 4A and 4B), respectively.

Obviously, the DSC curve of the dried PNIPAM has no melting peak. The heat flow increases with the rising of temperature, especially for temperatures higher than 35°C. As both the heating rate and mass of PNIPAM are constant during the testing, the specific heat capacity of dried PNIPAM has the same variation trend toward temperature. The specific heat capacity of PNIPAM is different from common materials. TDC is affected by density, thermal conductivity and specific heat capacity. The density is of constant during the testing process, and the thermal conductivity is of proportional relationship with the product of TDC and specific heat capacity. Though the specific heat capacity differs from common material, the thermal conductivity is of linear relationship with temperature, which is the same with common materials.

Water changes to bound and immobilized water above lower critical solution temperature

The distribution of T_2 relaxation time according to the LF-NMR testing results for the PNIPAM hydrogel under different water content is shown in (Figures 5A and 5B). The peak of the curve represents the water type and ratio in the PNIPAM hydrogel. The peak T_{21} (0.01–1 ms), T_{22} (1–100 ms), and T_{23} (>100 ms) represent the bound water, immobilized water, and free water, respectively. The peak area ratio of different water content is shown in (Figure 5C).

It can be found that the water in PNIPAM hydrogel is always of two peak characteristics. When the water content of the PNIPAM is higher than 0.6 g/g, the distribution of water type is mainly immobilized water and free water. For water content lower than 0.6 g/g, the water types are mainly immobilized water and bound water. When the water content is higher than 2.0 g/g, the water desorption manifests as the reduction of both free water and immobilized water, without changing for water type. With the further reduction of water content, the peaks of the curve gradually convert to immobilized water from free water and to bound water from immobilized water. During the desorption processes, the ratio of free water decreases, while the ratio of immobilized water and bound water increases. Thus, the water release gets more difficult with the proceeding of the desorption process.

The desorption will begin from the outer layer, and the pore of the PNIPAM skeleton will shrink. The reduction of the pore diameter of the outer layer will result in an obstructive effect for water releasing from the internal layer. For further analyzing of the dynamic of the water desorption process, the sample with a water content of 2.5 g/g was heated to higher than the LCST, and LF-NMR testing was conducted every few minutes, during the consecutive heating process. During the dynamic desorption process, the distribution of T_2 relaxation time according to the LF-NMR testing results of the PNIPAM hydrogel is shown in (Figures 6A and 6B).

It can be found that both the free water peak and immobilized water peak of the T_2 curve reduce at the beginning of the heating process, when the temperature of PNIPAM is higher than the LCST. The free water tends to convert to immobilized water, and the immobilized water changes to bound water. When heated for further, from 1 min to 8 min, the corresponding T_2 time and area ratio of the bound water do not change with the heating time. In comparison, T_2 time of the immobilized water peak reduces, and the area ratio of immobilized water increases with the increase of heating time. Thus, the shrinkage of the PNIPAM skeleton will leads to significant water type transformation, and the heating to the water releasing process will be hindered by the characteristic. On the other hand, the water type conversion trend of the dynamic heating process shows uniformity with steady state results.

Desorption in closed and air convection environment

Liquid water accounts for the vast majority in closed environment desorption

In closed environment, the evaporated water amount, from liquid to vapor, increases with the rising of heating temperature. There exists a maximum evaporated water amount in a closed environment, and the amount is also increases with the rising of the heating temperature. The time for reaching the saturated water vapor is lower than 60 min. Based on the quantification testing results of the evaporation amount, the water desorption amount as vapor type can be calculated. The testing results of liquid, vapor, and evaporation amounts during the PNIPAM dynamic desorption process are shown in (Figure 7A). During the heating

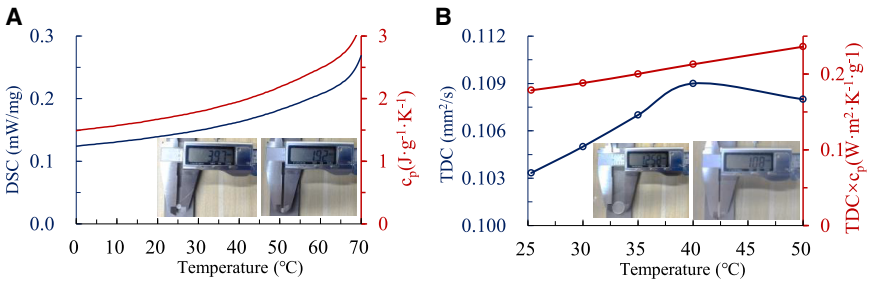

Figure 4. Thermal properties of dry PNIPAM

(A) DSC testing results. Data are represented as the result of single experiment.

(B) TDC testing results. Data are represented as the mean of three independent experiments.

process, the process that temperature of the PNIPAM increases to above the LCST will take several minutes. The beginning time, as soon as the PNIPAM transferred from transparent to opaque, is recorded as t_0. The ratio of different water desorption types for t_0 +600 s and t_0 +2400 s is listed later in discussion, as (Figure 7B) shows.

Obviously, the total desorption rate decreases with time going by. After 40 min desorption (T > LCST), the desorption rate tends to be stable and slow. The highest liquid water desorption amount occurs at a heating temperature of 50°C, about 0.30 g/g. The remaining water of the PNIPAM is 2.2 g/g, significantly higher than the desorbed water. When the temperature further increases to 60°C, the liquid water desorption amount decreases to 0.23 g/g. However, at the beginning of 5 min, the liquid water desorption amount of 60°C is higher than that of 40°C and 50°C heating temperature. This phenomenon may be attributed to the fast water release of the outer layer at the beginning of several minutes under high temperatures. When heated further, the fast shrinkage of the PNIPAM skeleton at the outer layer will block the internal water release for the following desorption process. In a closed environment, most of the water is desorbed as liquid water. Direct water vapor desorption from PNIPAM only takes about 10% of the total desorption amount. The rate of the evaporated water vapor and direct vapor desorption rate decreases sharply, due to the gradual saturation of the closed environment.

In brief, a heating temperature of 50°C is suitable for the conditions that a high liquid water amount is required, to obtain as much liquid water as possible. While for fast liquid water generation scenarios, high temperature (higher than 60°C) is better to obtain more liquid water within 5 min.

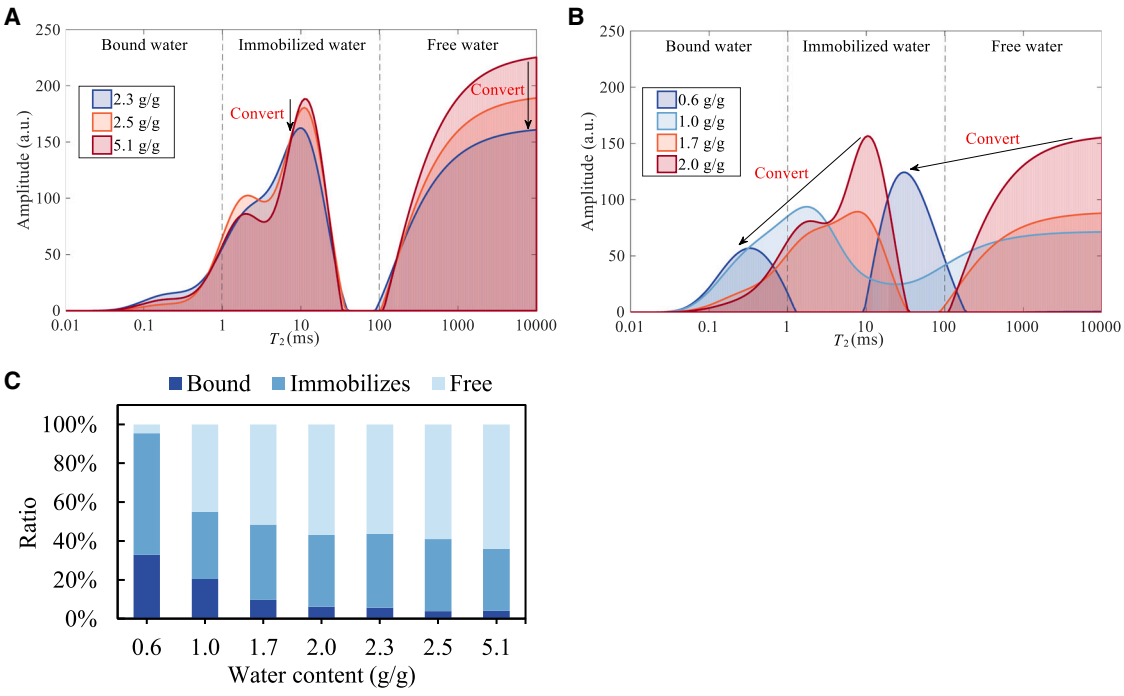

Figure 5. LF-NMR testing results for PNIPAM hydrogel under different water content

For water content higher than 2.0 g/g, the water desorption manifests as the reducing of both free water and immobilized water, without changing for water type. With the further reduction of water content, the peaks of the curve convert to immobilized water from free water and to bound water from immobilized water.

(A) T_2 curve for water content varies from 2.3 g/g to 5.1 g/g. Data are represented as the result of single experiment.

(B) T_2 curve for water content varies from 0.6 g/g to 2.0 g/g. Data are represented as the result of single experiment.

(C) The ratio of water type for different water content. Data are represented as the result of single experiment.

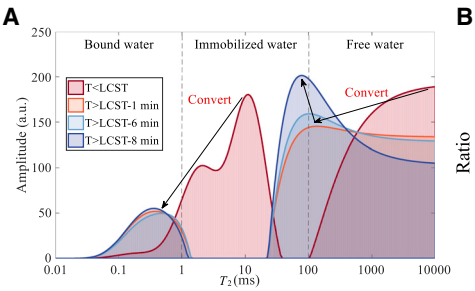

Figure 6. LF-NMR testing results for dynamic heating process of the PNIPAM hydrogel.Free water converts to immobilized water, and immobilized water changes to bound water, obstructing the water desorption process

(A) T_2 curve for different heating time. Data are represented as the result of single experiment.

(B) The ratio of water type for different desorption time. Data are represented as the result of single experiment.

High total desorption amount with low liquid water ratio in air convection environment

In air convection environment, the evaporated liquid water will not get saturated, and the water vapor can be taken away by the air flow. Under the same hot air temperature of 40°C–60°C, the liquid-vapor desorption performance of PNIPAM was tested. The air flow velocity was controlled at 2 m/s. The experimental results are shown in (Figures 8A and 8B, 8C and 8D).

During the convection heating process, the phase transition occurs along the flow direction of the hot air. Thus, the desorption can be divided into three stages, see (Figure 8A): transparent stage (T < LCST), transition stage (T > LCST for part of the material), and opaque stage (T > LCST). The liquid water and gaseous water have different desorption performances in the three stages, and (Figure 8B) shows the water desorption curve under different convection air temperature. For stage I, all the desorbed water is of gaseous type. When the phase transition of PNIPAM occurs, stage II, liquid water can be found. Due to the convection of hot air, most of the desorbed liquid water evaporates to water vapor. It can be found that the highest available liquid water (liquid water can be collected directly) is at the beginning of stage III. The reason is that the liquid water desorption rate decreases when the phase transition of the whole material is finished. When the liquid water desorption rate is lower than the evaporation rate, the available liquid water amount gets reduced.

To obtain the highest liquid water collection amount, a high convection air temperature is recommended. For air temperature ranges from 40°C to 60°C, the condition of 60°C has the highest available liquid water amount of about 0.11 g/g and fastest water desorption rate (10 min), see (Figure 8C). On the other hand, the air temperature of 60°C also has the highest total desorption amount, about 0.54 g/g. However, the amount of the available liquid water for air convection conditions is much lower than that for closed environment conditions. (Figure 8D) shows the ratio of available liquid water and the gaseous water under different desorption temperatures. The maximum available liquid water only takes

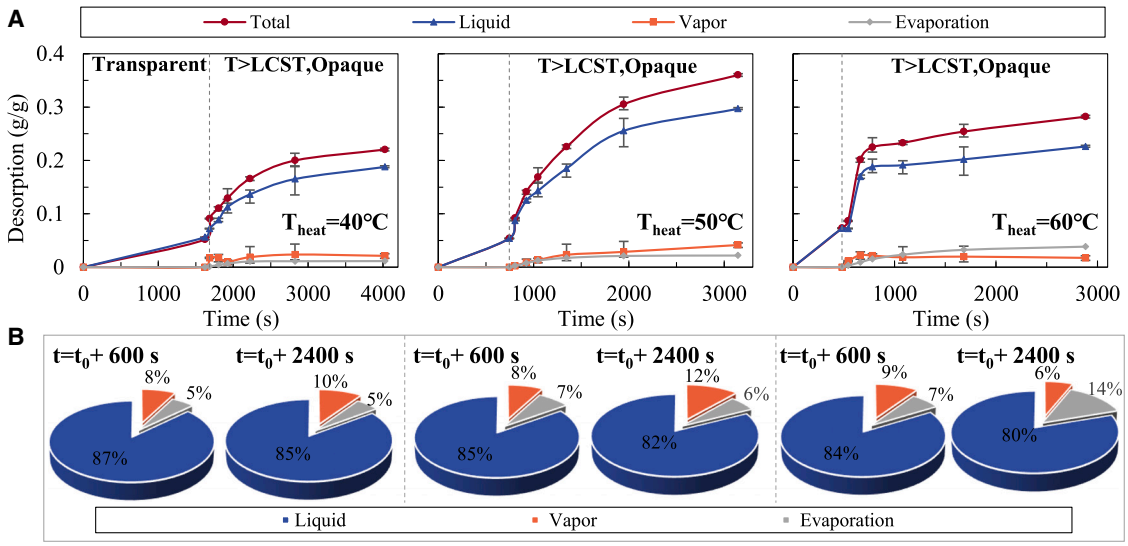

Figure 7. Liquid water and water vapor desorption of PNIPAM hydrogel in closed environment

50°C heating temperature has the highest desorption amount. Directly liquid water desorption takes more than 80% of the total desorption amount.

(A) Dynamic desorption curve of liquid water, vapor and evaporation under heating temperature of 40°C–60°C. Data are represented as mean, maximum and minimum value of three independent experiments.

(B) The corresponding desorbed water ratio under typical desorption time for different heating temperature. Data are represented as mean of three independent experiments.

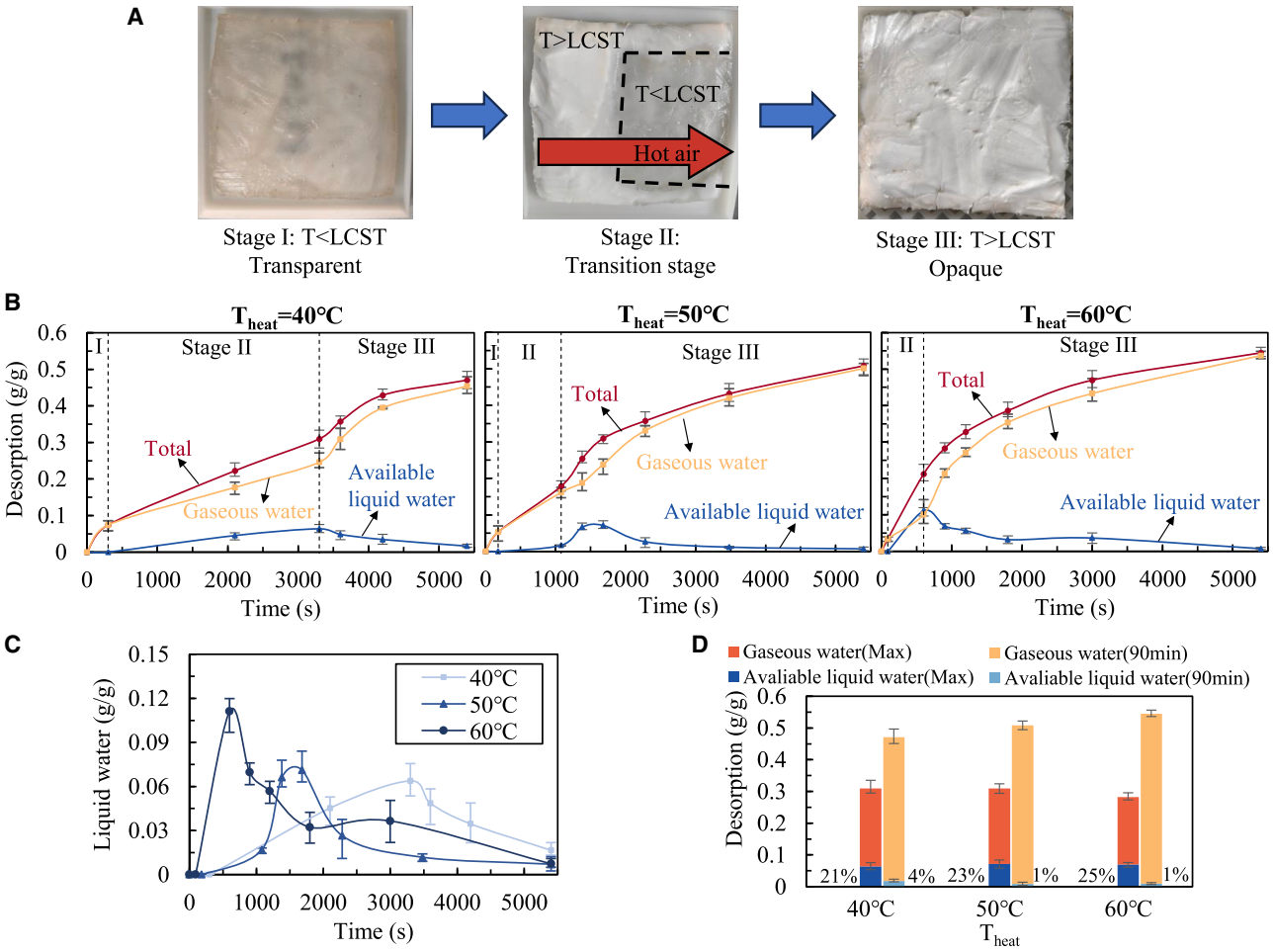

Figure 8. Liquid water and water vapor desorption of PNIPAM hydrogel under air convection condition

60°C has the highest total desorption amount, and the maximum available liquid water only takes 21%–25% of the total desorption amount.

(A) Three stages during the air convection desorption period.

(B) Available liquid water and gaseous water dynamic desorption curve of desorption air temperature ranges from 40°C to 60°C. Data are represented as mean, maximum and minimum value of three independent experiments.

(C) Liquid water capture comparison of three heating temperature. Data are represented as mean, maximum and minimum value of three independent experiments.

(D) Liquid and gaseous water desorption ratio under heating time of maximum liquid water amount and 90 min. Data are represented as mean, maximum and minimum value of three independent experiments.

21%–25% of the total desorption amount. Thus, to obtain more liquid water, the combination of condensation equipment is necessary, for the air convection conditions.

DISCUSSION

Obviously, the desorption and liquid water releasing process of the PNIPAM hydrogel will be restricted by the shrinkage of the outer layer, for both closed environment and air convection environment. The liquid water desorption mechanism is attributed to the shrinkage of the PNIPAM polymer chain. When the transfusion of the liquid water is blocked by the low pore diameter and low porosity of the outer layer, the following desorption will be in the form of water vapor. Both heating temperature and heating rate affect the water releasing performance, during the heating process. In this research, heating rate relates to the product of air flowrate and air temperature. By increasing the heating rate, from about 38.5 W to 57.6 W, the total water release amount and release speed increases. From the perspective of direct liquid water amount, increasing heating rate benefits to water collection capacity and efficiency, within 600 s of 0.11 g/g. The kinetic reason is the fast transition of PNIPAM and the shorten of stage I and stage II. A low heating rate causes a large amount of outer layer water to diffuse as gaseous type, reducing the liquid water releasing amount when heated to above the LCST. Thus, improving the heating rate to shorten the transition process contributes to obtain liquid water. On the other hand, a higher heating rate provides more energy for both the transition of PNIPAM and water evaporation, increasing the total water releasing amount.

Another key factor is the geometric parameter, including length alongside the air stream and thickness. Reducing the

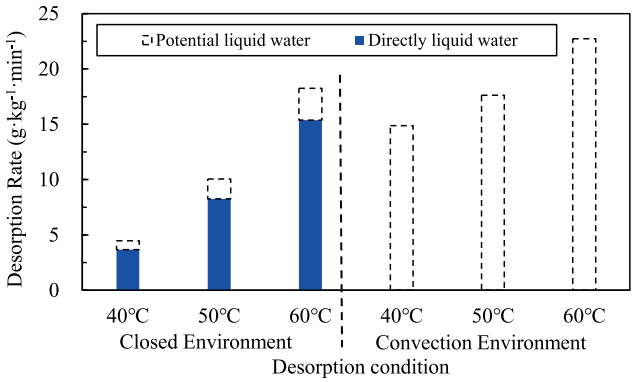

Figure 9. Liquid water and potential liquid water generation rate of different conditions

The highest directedly liquid water desorption rate is in a closed environment, and the highest potential liquid water desorption rate is for air convection condition, with the requirement of excess cooling condensation equipment. Data are represented as mean of three independent experiments.

length of PNIPAM alongside the air stream can shorten the transition stage (stage II) of the air convection condition, reducing the amount of water diffused as a gaseous type. Based on the theory of water transfusion in porous media, water flux density increases with the rising of pore diameter and the reducing of transfusion length. From this point of view, the thinner polymer has a shorter transfusion length. On the other hand, the thinner polymer has a shorter heat transfer time, from surface to interior. When the temperature at the center point increases to above the LCST, the pore diameter at the outermost layer of thinner PNIPAM is larger than that of thicker PNIPAM, which may cause greater water flux density. Thus, when heated to above the LCST, driven by the force of molecular chain shrinkage, thin polymer may be conducive to the collection of water.

Consecutive heating method may not be suitable for the conditions requiring high liquid water collection amount. To solve this problem, intermittent heating and desorption by changing the temperature of PNIPAM hydrogel may be a potential solution method. After heating to above the LCST for several minutes, the hydrogel can be purged with low temperature environment air for several minutes to uniform the water content of the whole hydrogel. For further, the establishment of the heat and mass transfer model for describing the two-phase desorption performance of TRPs is highly recommended. Based on the water transfusion law inside TRPs, the cycle time of heating and purging with ambient air can be optimized. In addition to the operation strategy, changing the micro structure of hydrogel during water releasing process through active adjustment,[58] is a potential method to reduce the blocking effect of pore diameter reduction. On the other hand, by spraying hydrophobic film[59] between different PNIPAM layers can effectively reduce the water diffusion distance, improving water collection efficiency. For some specific pollutants, the water recovery efficiency can be improved by coupling with other technologies, e.g., pseudocapacitance system for removing rare-earth ions in waste water.[60]

Based on the desorption performance of PNIPAM under two environments, the liquid water generation amount and rate can be concluded. There is no doubt that the highest liquid water amount (directly obtained without further process) is for the 50°C in closed environment, 0.3 g/g for heating to about 53 min. However, the liquid water generation rate of this condition is not high, only 5.7 g $kg^{-1}\cdot min^{-1}$. The highest liquid water generation rate is for 60°C in a closed environment, see (Figure 9). The liquid water can be generated directly at a rate of 15.4 g $kg^{-1}\cdot min^{-1}$ by heating at 60°C for 11 min, 2.7 times higher than that of the highest liquid water amount condition. By combining with a water vapor condenser, the theoretical liquid water generation rate turns to 18.2 g $kg^{-1}\cdot min^{-1}$. Compared with desorption in a closed environment, air convection environment can reach 22.7 g $kg^{-1}\cdot min^{-1}$ by heating at 60°C for 1.5 min. It seems that this condition has the highest total water desorption rate (potential liquid water), the cooling energy is high due to the condensation of gaseous water requirement. Thus, three desorption strategies of PNIPAM based thermal-responsive polymers can be recommended for different purified water generation requirements. For scenarios with high liquid water generation amount, 50°C in a closed environment is recommended. When the requirement is fast water purification, intermittent

Table 1. The comparison of the water generation among previously researches

Reference	Polymer type	Water desorption
This research	PNIPAM	22.7 g/(kg·min), in 1.5 min, 60°C 15.4 g/(kg·min) (liquid), in 11 min, 60°C
Ma et al.[9]	PNIPAM-Silica gel-LiCl	0.7 g/g in 30 min, 40°C
Zhao et al.[55]	IPN of PNIPAM and PPy-Cl	3.4 g/g in 20 min, 40°C
Nandakumar et al.[61]	Gel made by Zn from its acetate salt combined with an alcohol, anamino-alcohol and water.	14 L/(kg·day) = 9.72 g/(kg·min), 50°C
Hanikel et al.[62]	MOF-303	1.3 kg/(kg·day) = 0.90 g/(kg·min), 120°C
Yao et al.[63]	PAAS/GO	25 kg/(kg·day) = 17.36 g/(kg·min), 60°C
Ji et al.[64]	MCM-41/$CaCl_2$	1.2 kg/(kg·day) = 0.83 g/(kg·min), 80°C
Cai et al.[65]	IPN of PNIPAM and PVA	0.23 L/(m^2·h), 40°C
Geng et al.[66]	PNIPAM anchored onto a superhydrophilic melamine foam skeleton, with modified graphene layer	4.2 kg/(m^2·h), 43°C, 99% ionic rejection

heating at 60°C in a closed environment can achieve a high liquid water generation rate (heating for 11 min and cooling for several minutes). If the energy consumption is not considered, intermittent heating at 60°C with air convection can be adopted (heating for 1.5 min and cooling for several minutes), by using a condenser to obtain liquid water from gaseous water.

(Table 1) shows a comparison of this research and previously reported researches, in terms of water purification and generation performance. It can be found that the PNIPAM in the current research has a relative high water desorption rate compared with previously reported researches, of 15.4 g $kg^{-1}\cdot min^{-1}$ directly liquid water generation rate and 22.7 g $kg^{-1}\cdot min^{-1}$ water generation rate with further condensation.

Conclusions

In this research, combined micro and macro methods were adopted to analyze both dynamic structural parameters and liquid-vapor water releasing, for a PNIPAM hydrogel. On the basis of experimental testing, several main findings were concluded. With the water content increases to the maximum adsorption amount, the pore diameter increases, and the micro surface gets rough. The bulk volume is of linear relationship with the variation of water content, and the average CME is 0.94 m^3/kg. Based on LF-NMR characterization, PNIPAM shows a two-peak feature under T_2 relaxation. Free and immobilized water is transferred to immobilized and bound water, for water content reduces from 2.0 g/g to 0.6 g/g and during the dynamic heating process. The highest liquid water directly collection amount is for the 50°C in closed environment, 0.3 g/g for heating to about 53 min. The highest liquid water generation rate is 15.4 g $kg^{-1}\cdot min^{-1}$, in a closed environment by heating at 60°C for 11 min. By combining with a water vapor condenser, the theoretical liquid water generation rate turns to 18.2 g $kg^{-1}\cdot min^{-1}$. Compared with desorption in a closed environment, air convection environment can reach 22.7 g $kg^{-1}\cdot min^{-1}$ by heating at 60°C for 1.5 min. In general, PNIPAM hydrogel is a potential water purification material, while the optimization of geometry parameters and heating strategies is highly recommended for the improvement of energy and water collection efficiency.

Limitations of the study

In this research, we emphasize on the liquid and vapor desorption performance of a typical thermal-responsive polymer PNIPAM. Other kinds of thermal-responsive polymers could have been experimented. This research conducted micro and macro experimental methods for the water desorption performance of PNIPAM. A comprehensive liquid water purification and generation strategies could be proposed from the establishment of a general physical model of thermal-responsive polymers. The shape factors, e.g., length, width, and thickness, along with the intermittent heating-cooling method could be optimized for obtaining a high liquid water generation rate.

RESOURCE AVAILABILITY

Lead contact

Requests for further information and resources should be directed to and will be fulfilled by the lead contact, Xing Su (suxing@tongji.edu.cn).

Materials availability

This study did not generate new unique reagents.

Data and code availability

- All data reported in this article will be shared by the lead contact upon request.
- This article does not report original code.
- Any additional information required to reanalyze the data reported in this article is available from the lead contact upon request.

ACKNOWLEDGMENTS

This research is supported by the National Natural Science Foundation of China under grant No. 52178085, the Fundamental Research Funds for the Central Universities under grant No. 22120220645 and the Shanghai Professional Technical Service Platform of Smart and Low-Carbon Controlled Built Environment under grant No. 23DZ2290100.

AUTHOR CONTRIBUTIONS

Conceptualization, S.T. and X.S.; methodology, S.T.; data curation, L. H.; investigation, S.T. and C.C.; formal analysis, S. T.; validation, C.C.; resources, X. Y. and A. S.; writing-original draft, S.T.; writing-review and editing, X.S.; supervision, X.S.; project administration, X.S.; funding acquisition, X.S. All authors have read, edited, and approved the final article.

DECLARATION OF INTERESTS

The authors declare no competing interests.

STAR★METHODS

Detailed methods are provided in the online version of this paper and include the following:

- KEY RESOURCES TABLE
- METHOD DETAILS
  - Synthesis of typical TRP PNIPAM
  - Characterization of PNIPAM
  - Liquid-vapor desorption experiment
- QUANTIFICATION AND STATISTICAL ANALYSIS

SUPPLEMENTAL INFORMATION

Supplemental information can be found online at https://doi.org/10.1016/j.isci.2024.111619.

Received: August 22, 2024
Revised: November 21, 2024
Accepted: December 14, 2024
Published: December 18, 2024

REFERENCES

1. Xu, X., Bizmark, N., Christie, K.S.S., Datta, S.S., Ren, Z.J., and Priestley, R.D. (2022). Thermoresponsive polymers for water treatment and collection. Macromolecules (Washington, DC, U. S.) *55*, 1894–1909. https://doi.org/10.1021/acs.macromol.1c01502.
2. Zhang, C., Liang, H.-Q., Xu, Z.-K., and Wang, Z. (2019). Harnessing solar-driven photothermal effect toward the water–energy nexus. Adv. Sci. *6*, 1900883. https://doi.org/10.1002/advs.201900883.
3. El-Sewify, I.M., and Ma, S. (2024). Recent development of metal-organic frameworks for water purification. Langmuir *40*, 5060–5076. https://doi.org/10.1021/acs.langmuir.3c03818.
4. Li, M., Guo, H., Xiao, Y., Liu, S., Lu, Y., Wang, L., and James, T.D. (2024). Super stable evaporators based on upcycled self-healing adsorbents for

wastewater regeneration. Environ. Sci.: Nano *11*, 1271–1282. https://doi.org/10.1039/d3en00829k.

5. Al-Gethami, W., Qamar, M.A., Shariq, M., Alaghaz, A.N.M.A., Farhan, A., Areshi, A.A., and Alnasir, M.H. (2024). Emerging environmentally friendly bio-based nanocomposites for the efficient removal of dyes and micropollutants from wastewater by adsorption: a comprehensive review. RSC Adv. *14*, 2804–2834. https://doi.org/10.1039/d3ra06501d.
6. Yoon, J.H., Kim, T., Seo, M., and Kim, S.Y. (2024). Synthesis and thermoresponsive behavior of poly(N-isopropylacrylamide)-b-poly(N-vinylisobutyra mide) diblock copolymer. Polymers *16*, 830. https://doi.org/10.3390/polym16060830.
7. Li, C., Luo, Z., Qing, S., Wang, Y., Huang, H., and Zhang, X. (2024). Investigation of nanocomposite PNIPAm-g-graphene with pre-lower critical solution temperature rapid thermal response function for chip adaptive cooling: A molecular dynamics and computational fluid dynamics simulations. J. Polym. Sci. *62*, 1934–1951. https://doi.org/10.1002/pol.20230725.
8. Kim, S., and Choi, H. (2019). Switchable wettability of thermoresponsive core–shell nanofibers for water capture and release. ACS Sustain. Chem. Eng. *7*, 19870–19879. https://doi.org/10.1021/acssuschemeng.9b05273.
9. Ma, Q., and Zheng, X. (2022). Preparation and characterization of thermoresponsive composite for adsorption-based dehumidification and water harvesting. Chem. Eng. J. *429*, 132498. https://doi.org/10.1016/j.cej.2021.132498.
10. Karmakar, A., Mileo, P.G.M., Bok, I., Peh, S.B., Zhang, J., Yuan, H., Maurin, G., and Zhao, D. (2020). Thermo-responsive MOF/polymer composites for temperature-mediated water capture and release. Angew. Chem. Int. Ed. *59*, 11003–11009. https://doi.org/10.1002/anie.202002384.
11. Zha, X., Hao, Y., Ke, Y., Wang, Y., and Zhang, Y. (2024). Berberine-loaded PVCL-PVA-PEG self-assembled micelles for the treatment of liver fibrosis. Int. J. Nanomed. *19*, 10857–10872. https://doi.org/10.2147/ijn.s465214.
12. Takatsuka, M., Arai, Y., Sasaki, K., Kita, R., Yagihara, S., and Shinyashiki, N. (2024). Dielectric relaxations of polymer and primary and slow water in water mixtures of poly(vinyl methyl ether) as a polymer with low glass transition temperature. Macromolecules (Washington, DC, U. S.) *57*, 8338–8350. https://doi.org/10.1021/acs.macromol.4c00616.
13. Wu, Z., Wang, Z., Li, J., Chen, W., and Zhang, Z. (2024). Cotton fiber coated with a novel lysozyme-polymer brush conjugates for efficient oil-water separation. Mater. Today Commun. *40*, 109837. https://doi.org/10.1016/j.mtcomm.2024.109837.
14. Mfoafo, K., Omidi, Y., and Omidian, H. (2023). Thermoresponsive mucoadhesive hybrid gels in advanced drug delivery systems. Int. J. Pharm. *636*, 122799. https://doi.org/10.1016/j.ijpharm.2023.122799.
15. Lacroce, E., and Rossi, F. (2022). Polymer-based thermoresponsive hydrogels for controlled drug delivery. Expet Opin. Drug Deliv. *19*, 1203–1215. https://doi.org/10.1080/17425247.2022.2078806.
16. Chen, S., Li, Y., Feng, Y., and Feng, W. (2023). Thermally responsive polymers for overcoming thermal runaway in high-safety electrochemical storage devices. Mater. Chem. Front. *7*, 1562–1590. https://doi.org/10.1039/d2qm01342h.
17. Ji, Y., Sun, Y., Javed, M., Xiao, Y., Li, X., Jin, K., Cai, Z., and Xu, B. (2022). Skin inspired thermoresponsive polymer for constructing self-cooling system. Energy Convers. Manag. *254*, 115251. https://doi.org/10.1016/j.enconman.2022.115251.
18. Zhang, Y., Wang, W., Zheng, X., and Cai, J. (2024). Recent progress on composite desiccants for adsorption-based dehumidification. Energy *302*, 131824. https://doi.org/10.1016/j.energy.2024.131824.
19. Muralter, F., Greco, F., and Coclite, A.M. (2020). Applicability of vapor-deposited thermoresponsive hydrogel thin films in ultrafast humidity sensors/actuators. ACS Appl. Polym. Mater. *2*, 1160–1168. https://doi.org/10.1021/acsapm.9b00957.
20. Vihola, H., Laukkanen, A., Valtola, L., Tenhu, H., and Hirvonen, J. (2005). Cytotoxicity of thermosensitive polymers poly(N-isopropylacrylamide), poly(N-vinylcaprolactam) and amphiphilically modified poly(N-vinylcaprolactam). Biomaterials *26*, 3055–3064. https://doi.org/10.1016/j.biomaterials.2004.09.008.
21. Lutz, J.-F. (2008). Polymerization of oligo(ethylene glycol) (meth)acrylates: Toward new generations of smart biocompatible materials. J. Polym. Sci. A. Polym. Chem. *46*, 3459–3470. https://doi.org/10.1002/pola.22706.
22. Zhang, K., Li, F., Wu, Y., Feng, L., and Zhang, L. (2020). Construction of ionic thermo-responsive PNIPAM/γ-PGA/PEG hydrogel as a draw agent for enhanced forward-osmosis desalination. Desalination *495*, 114667. https://doi.org/10.1016/j.desal.2020.114667.
23. Jian, Z., Shuang, C., Qingyang, W., and Renkun, C. (2019). Multi-layer temperature-responsive hydrogel for forward-osmosis desalination with high permeable flux and fast water release. Desalination *459*, 105–113. https://doi.org/10.1016/j.desal.2019.02.002.
24. Xia, L.W., Xie, R., Ju, X.J., Wang, W., Chen, Q., and Chu, L.Y. (2013). Nano-structured smart hydrogels with rapid response and high elasticity. Nat. Commun. *4*, 2226. https://doi.org/10.1038/ncomms3226.
25. Fei, R., George, J.T., Park, J., Means, A.K., and Grunlan, M.A. (2013). Ultra-strong thermoresponsive double network hydrogels. Soft Matter *9*, 2912–2919. https://doi.org/10.1039/c3sm27226e.
26. Zhang, W., Liu, N., Zhang, Q., Qu, R., Liu, Y., Li, X., Wei, Y., Feng, L., and Jiang, L. (2018). Thermo-driven controllable emulsion separation by a polymer-decorated membrane with switchable wettability. Angew. Chem. Int. Ed. *57*, 5740–5745. https://doi.org/10.1002/anie.201801736.
27. Gong, Z., Li, S., Ma, J., and Zhang, X. (2016). Self-flocculated powdered activated carbon with different oxidation methods and their influence on adsorption behavior. J. Hazard Mater. *304*, 222–232. https://doi.org/10.1016/j.jhazmat.2015.10.039.
28. Kubota, M., Mochizuki, T., Yamashita, S., Kita, H., and Tokuyama, H. (2020). Water vapor adsorption on poly(N-isopropylacrylamide) gel cross-linked with N, N′-methylenebisacrylamide. Mater. Today Commun. *22*, 100804. https://doi.org/10.1016/j.mtcomm.2019.100804.
29. Kazuya, M., Nobuki, S., and Takashi, M. (2018). Thermo-responsive gels that absorb moisture and ooze water. Nat. Commun. *9*, 2315. https://doi.org/10.1038/s41467-018-04810-8.
30. Zhao, F., Zhou, X., Liu, Y., Shi, Y., Dai, Y., and Yu, G. (2019). Super moisture-absorbent gels for all-weather atmospheric water harvesting. Adv. Mater. *31*, e1806446. https://doi.org/10.1002/adma.201806446.
31. Rana, A., and Wang, R.Y. (2024). Thermoresponsive liquid desiccants for dehumidification cycles. Energy Convers. Manag. *301*, 118029. https://doi.org/10.1016/j.enconman.2023.118029.
32. Gadore, V., and Ahmaruzzaman, M. (2021). Smart materials for remediation of aqueous environmental contaminants. J. Environ. Chem. Eng. *9*, 106486. https://doi.org/10.1016/j.jece.2021.106486.
33. Reddy, A.S., Wanjari, V.P., and Singh, S.P. (2023). Design, synthesis, and application of thermally responsive draw solutes for sustainable forward osmosis desalination: A review. Chemosphere *317*, 137790. https://doi.org/10.1016/j.chemosphere.2023.137790.
34. Li, D., Zhang, X., Yao, J., Simon, G.P., and Wang, H. (2011). Stimuli-responsive polymer hydrogels as a new class of draw agent for forward osmosis desalination. Chem. Commun. *47*, 1710–1712. https://doi.org/10.1039/C0CC04701E.
35. Li, D., Zhang, X., Yao, J., Zeng, Y., Simon, G.P., and Wang, H. (2011). Composite polymer hydrogels as draw agents in forward osmosis and solar dewatering. Soft Matter *7*, 10048. https://doi.org/10.1039/C1SM06043K.
36. Zeng, J., Cui, S., Wang, Q., and Chen, R. (2019). Multi-layer temperature-responsive hydrogel for forward-osmosis desalination with high permeable flux and fast water release. Desalination *459*, 105–113. https://doi.org/10.1016/j.desal.2019.02.002.
37. Wang, L., Wang, G., Di, Y., Wang, H., Wang, P., Dong, L., Huang, Y., and Jin, G. (2024). Fast reversion of hydrophility-superhydrophobicity on

textured metal surface by electron beam irradiation. Appl. Surf. Sci. *669*, 160455. https://doi.org/10.1016/j.apsusc.2024.160455.

38. Fan, S., Li, Z., Fan, C., Chen, J., Huang, H., Chen, G., Liu, S., Zhou, H., Liu, R., Feng, Z., et al. (2022). Fast-thermoresponsive carboxylated carbon nanotube/chitosan aerogels with switchable wettability for oil/water separation. J. Hazard Mater. *433*, 128808. https://doi.org/10.1016/j.jhazmat.2022.128808.
39. Wang, H.L., Liu, L.Y., Kou, W.Q., and Jiang, W.F. (2013). Preparation of thermosensitive and visible-light responsible composites based on hydrogels of N-isopropylacrylamide/maleic anhydride-modified β-cyclodextrin copolymer and TiO_2 multiwalled carbon nanotubes particles for degradation of methyl orange. Polym. Compos. *34*, 681–689. https://doi.org/10.1002/pc.22471.
40. Graillot, A., Djenadi, S., Faur, C., Bouyer, D., Monge, S., and Robin, J.J. (2013). Removal of metal ions from aqueous effluents involving new thermosensitive polymeric sorbent. Water Sci. Technol. *67*, 1181–1187. https://doi.org/10.2166/wst.2013.671.
41. Wang, W., Liu, Z., Wang, R., Cao, M., Chen, Y., Lu, X., Ma, H., Yue, T., and Yan, T. (2023). A novel strategy for efficient removal of hazardous metal ions based on thermoresponsive phase separation of the PNIPAM/GO system. Chem. Eng. J. *470*, 143967. https://doi.org/10.1016/j.cej.2023.143967.
42. Sharma, R., Haldar, U., Turabee, M.H., and Lee, H.I. (2021). Recyclable macromolecular thermogels for Hg(II) detection and separation via sol-gel transition in complex aqueous environments. J. Hazard Mater. *410*, 124625. https://doi.org/10.1016/j.jhazmat.2020.124625.
43. Singh, S., and Jelinek, R. (2020). Sunlight-activated phase transformation in carbon dot-hydrogel facilitates water purification and optical switching. ACS Appl. Polym. Mater. *2*, 2810–2818. https://doi.org/10.1021/acsapm.0c00358.
44. Xu, X., Ozden, S., Bizmark, N., Arnold, C.B., Datta, S.S., and Priestley, R.D. (2021). A bioinspired elastic hydrogel for solar-driven water purification. Adv. Mater. *33*, 2007833. https://doi.org/10.1002/adma.202007833.
45. Xu, X., Guillomaitre, N., Christie, K.S.S., Bay, R.K.N., Bizmark, N., Datta, S.S., Ren, Z.J., and Priestley, R.D. (2023). Quick-release antifouling hydrogels for solar-driven water purification. ACS Cent. Sci. *9*, 177–185. https://doi.org/10.1021/acscentsci.2c01245.
46. Joe, J.H., Park, J.M., Lee, H., and Jang, W.D. (2019). A dendritic-linear block copolymer as a thermoresponsive non-ionic polymer surfactant. Eur. Polym. J. *118*, 320–326. https://doi.org/10.1016/j.eurpolymj.2019.06.007.
47. Combita, D., and Ahmed, M. (2021). Thermoresponsive and antifouling hydrogels as a radiative energy driven water harvesting system. Mater. Chem. Front. *5*, 917–928. https://doi.org/10.1039/d0qm00584c.
48. Hyk, W., and Kitka, K. (2018). Water purification using sponge like behaviour of poly (N-isopropylacrylamide) ferrogels. Studies on silver removal from water samples. J. Environ. Chem. Eng. *6*, 6108–6117. https://doi.org/10.1016/j.jece.2018.09.027.
49. Kafetzi, M., Borchert, K.B., Steinbach, C., Schwarz, D., Pispas, S., and Schwarz, S. (2021). Thermoresponsive PNIPAM-b-PAA block copolymers as "smart" adsorbents of Cu(II) for water restore treatments. Colloids Surf., A *614*, 126049. https://doi.org/10.1016/j.colsurfa.2020.126049.
50. Takahashi, T., Yoshida, T., Tanaka, M., Ichikawa, T., Ohno, H., and Nakamura, N. (2024). Control of phase transition temperature of thermoresponsive poly(ionic liquid) gels and application to a water purification system using these gels with polydopamine. Sep. Purif. Technol. *337*, 126433. https://doi.org/10.1016/j.seppur.2024.126433.
51. Sanchez-Ferrer, A., Kotharangannagari, V.K., Ruokolainen, J., and Mezzenga, R. (2013). Thermo-responsive peptide-based triblock copolymer hydrogels. Soft Matter *9*, 4304–4311. https://doi.org/10.1039/c3sm27690b.
52. Kollofrath, D., Krysiak, Y., and Polarz, S. (2023). Activatable multizone hybrid hydrogels containing porous organosilica nanoparticles as gatekeepers. Chem. Mater. *35*, 8406–8416. https://doi.org/10.1021/acs.chemmater.3c01125.
53. Liu, T., Zhao, G., Qu, B., and Gong, C. (2024). Characterization of a fly ash-based hybrid well cement under different temperature curing conditions for natural gas hydrate drilling. Construct. Build. Mater. *445*, 137874. https://doi.org/10.1016/j.conbuildmat.2024.137874.
54. Rai, M., Pandey, A., Singh, S.K., and Maiti, A. (2024). Thermo-responsive polymer to clean fouled forward osmosis membrane after wastewater treatment: Excellent flux recovery. Polym. Eng. Sci. *64*, 2541–2553. https://doi.org/10.1002/pen.26708.
55. Zhao, F., Zhou, X., Shi, Y., Qian, X., Alexander, M., Zhao, X., Mendez, S., Yang, R., Qu, L., and Yu, G. (2018). Highly efficient solar vapour generation via hierarchically nanostructured gels. Nat. Nanotechnol. *13*, 489–495. https://doi.org/10.1038/s41565-018-0097-z.
56. Zhang, Z., Wang, Y., Li, Z., Fu, H., Huang, J., Xu, Z., Lai, Y., Qian, X., and Zhang, S. (2022). Sustainable hierarchical-pored PAAS–PNIPAAm hydrogel with core–shell structure tailored for highly efficient atmospheric water harvesting. ACS Appl. Mater. Interfaces *14*, 55295–55306. https://doi.org/10.1021/acsami.2c19840.
57. Rana, M.M., Rajeev, A., Natale, G., and De la Hoz Siegler, H. (2021). Effects of synthesis-solvent polarity on the physicochemical and rheological properties of poly(N-isopropylacrylamide) (PNIPAm) hydrogels. J. Mater. Res. Technol. *13*, 769–786. https://doi.org/10.1016/j.jmrt.2021.05.009.
58. Xu, D., Meng, X., Liu, S., Poisson, J., Vana, P., and Zhang, K. (2024). Dehydration regulates structural reorganization of dynamic hydrogels. Nat. Commun. *15*, 6886. https://doi.org/10.1038/s41467-024-51219-7.
59. Li, X., Liu, Y., and Leng, J. (2023). Large-scale fabrication of superhydrophobic shape memory composite films for efficient anti-icing and de-icing. Sustainable Mater. Technol. *37*, e00692. https://doi.org/10.1016/j.susmat.2023.e00692.
60. Mao, M., Qi, Y., Lu, K., Chen, Q., Xie, X., Li, X., Lin, Z., Chai, L., and Liu, W. (2024). Selective capacitive recovery of rare-earth ions from wastewater over phosphorus-modified TiO2 cathodes via an electro-adsorption process. Environ. Sci. Technol. *58*, 14013–14021. https://doi.org/10.1021/acs.est.4c03241.
61. Nandakumar, D.K., Zhang, Y., Ravi, S.K., Guo, N., Zhang, C., and Tan, S.C. (2019). Solar energy triggered clean water harvesting from humid air existing above sea surface enabled by a hydrogel with ultrahigh hygroscopicity. Adv. Mater. *31*, 1806730. https://doi.org/10.1002/adma.201806730.
62. Hanikel, N., Prévot, M.S., Fathieh, F., Kapustin, E.A., Lyu, H., Wang, H., Diercks, N.J., Glover, T.G., and Yaghi, O.M. (2019). Rapid cycling and exceptional yield in a metal-organic framework water harvester. ACS Cent. Sci. *5*, 1699–1706. https://doi.org/10.1021/acscentsci.9b00745.
63. Yao, H., Zhang, P., Huang, Y., Cheng, H., Li, C., and Qu, L. (2020). Highly efficient clean water production from contaminated air with a wide humidity range. Adv. Mater. *32*, 1905875. https://doi.org/10.1002/adma.201905875.
64. Ji, J.G., Wang, R.Z., and Li, L.X. (2007). New composite adsorbent for solar-driven fresh water production from the atmosphere. Desalination *212*, 176–182. https://doi.org/10.1016/j.desal.2006.10.008.
65. Cai, Y., Shen, W., Loo, S.L., Krantz, W.B., Wang, R., Fane, A.G., and Hu, X. (2013). Towards temperature driven forward osmosis desalination using Semi-IPN hydrogels as reversible draw agents. Water Res. *47*, 3773–3781. https://doi.org/10.1016/j.watres.2013.04.034.
66. Geng, H., Xu, Q., Wu, M., Ma, H., Zhang, P., Gao, T., Qu, L., Ma, T., and Li, C. (2019). Plant leaves inspired sunlight-driven purifier for high-efficiency clean water production. Nat. Commun. *10*, 1512. https://doi.org/10.1038/s41467-019-09535-w.

STAR★METHODS

KEY RESOURCES TABLE

REAGENT or RESOURCE	SOURCE	IDENTIFIER
Chemicals, peptides, and recombinant proteins		
NIPAM	Shanghai Titan Scientific	CAS: 2210-25-5
MBA	Beijing Innochem Technology	CAS: 110-26-9
TEMED	Beijing Innochem Technology	CAS: 110-18-9
APS	Beijing Innochem Technology	CAS: 7727-54-0
DI water	Shanghai MACKLIN Biochemical Technology	CAS: 7723-18-5

METHOD DETAILS

Synthesis of typical TRP PNIPAM

Materials

The adopted chemicals includes N-isopropylacrylamide (NIPAM, 98%), N, N′-methylenebisacrylamide (MBA, 99%), ammonium persulphate (APS, ≥98%), N,N,N′,N′-tetramethylenediamine (TEMED, 99%) and deionized (DI) water. The NIPAM was purchased from Shanghai Titan Scientific Co., Ltd. Ammonium persulphate. The MBA, APS, and TEMED were purchased from Beijing Innochem Technology Co., Ltd. The DI water was purchased from Shanghai MACKLIN Biochemical Technology Co., Ltd.

Preparation of PNIPAM hydrogels

In a typical synthesis, NIPAM (1g) and TEMED (10 μL) were dissolved in 10 mL DI water under sonication (NIPAM solution). The solution was purged with nitrogen for 10 min to remove the dissolved oxygen. 200 μL MBA solution of 30 mg/mL acting as crosslinker and 50 μL APS solution of 225 mg/mL acting as initiator were added into the NIPAM solution under sonication. During the operation process, the NIPAM solution was immersed in ice water to maintain a lower temperature. The polymerization was carried out under temperature of 10-20°C for 24 h to obtain PNIPAM hydrogel. The PNIPAM hydrogel was placed in DI water at 10-20°C for 48 h to remove the unreacted monomers. The PNIPAM hydrogel was dried in a vacuum oven at 50°C to constant weight, and the dry weight of the PNIPAM hydrogel can be obtained. The schematic diagram for the synthesis process is shown in (Figure S1).

Characterization of PNIPAM

The characterization of PNIPAM hydrogel includes macro structure and micro porous parameters. The water content related macro structure can be reflected by coefficient of macro expansion. The micro porous parameters mainly include porosity and pore diameter distribution.

Surface morphology of PNIPAM hydrogel

PNIPAM hydrogel has water content related characteristics of both macro structure and micro porous parameters. To analyse the surface morphology of micro structure under different water content, the completely dried PNIPAM hydrogels were rehydrated to different water content of 0 g/g, 1 g/g, 2.2 g/g, 6.8 g/g and maximum water content. Then, the PNIPAM hydrogels were freeze-dried for 48 h under temperature of lower than -60°C to maintain the porous structure. The freeze-dried PNIPAM hydrogels were examined by scanning electron microscope (SEM). The adopted SEM is JSM-6510 of Japan Electronics Co., Ltd (JEOL).

Crystallinity study

X-ray diffraction (XRD) was adopted to characterize the crystallinity of the PNIPAM hydrogel. The completely dried thin plate sample (18 mm in length and width, 2 mm in thickness) was analyzed on the diffractometer of Rigaku-SmartLab in the 2θ range of 10°–80° with 5°/min scanning rate.

Gel fraction

During the swelling and shrinking processes of the PNIPAM hydrogel, the mass of the water affects the gel fraction. The gel fraction *GF* of PNIPAM hydrogel was estimated by (Equation 1).

$$GF = \frac{M_{dry,PNIPAM}}{M_{total,PNIPAM}} \times 100\% \quad \text{(Equation 1)}$$

where $M_{dry,PNIPAM}$ is the weight of the completely dried PNIPAM sample and $M_{total,PNIPAM}$ is the total weight of PNIPAM hydrogel under different water content.

Coefficient of macro expansion

The water content related macro volume expansion of the PNIPAM hydrogel can be reflected by the coefficient of macro expansion (CME). CME is defined as the ratio of water content volume and water content weight, which is expressed as (Equation 2).

$$CME = \frac{V_{hydro} - V_{dry}}{W_{hydro} - W_{dry}} \quad \text{(Equation 2)}$$

where CME is the coefficient of macro expansion, V_{hydro} and V_{dry} represent the PNIPAM volume under hydration and dry condition, W_{hydro} and W_{dry} represent the PNIPAM mass weight under hydration and dry condition.

The experiment of CME is conducted during the heating and vacuum drying processes. The volume and mass of the PNIPAM were tested after several hours drying till completely dried condition, from fully swollen state. The mass of the PNIPAM hydrogel was weighted by using the high precise electronic balance, and the volume was tested by using measuring cylinder with drainage method.

Thermal properties characterization

Differential scanning calorimetry (DSC) and thermal diffusion coefficient were used to characterizing the thermal performance of the completely dried PNIPAM. DSC testing was carried out using NETZSCH DSC 214 differential scanning calorimeter. The dried PNIPAM was prepared as a cylinder with a diameter of 3.97 mm and a thickness of 1.92 mm. The testing temperature ranges from 0°C to 70°C, with heating rate of 5°C/min. The protective atmosphere is nitrogen.

Thermal diffusion coefficient characterization of dried PNIPAM was conducted by using a laser thermal conductivity testing instrument of NETZSCH LFA 467. The dried PNIPAM was prepared as a thin plate with a diameter of 12.58 mm and a thickness of 1.08 mm. The tested temperature set point are 25°C, 30°C, 35°C, 40°C and 50°C. The protective atmosphere is nitrogen.

Liquid-vapor desorption experiment

LF-NMR measurements of the desorption process

LF-NMR testing results can reflect the water conditions in the PNIPAM hydrogel and the pore diameter distribution. In this research, LF-NMR is adopted for the water condition analyzation under different water content, and reflect the water condition transfer during heating process. LF-NMR testing was carried out using a NMRC12-010V-T NMR analyser with a magnetic field strength of 0.28±0.05 T and magnetic field uniformity of 300 ppm. The magnetic field stability is 300 Hz/hour, and the radio frequency field pulse frequency ranges from 2 MHz to 30 MHz. A series of PNIPAM samples of different water content were prepared (from 0.6 g/g to 5.1 g/g), and used for LF-NMR relaxation analysis. All the completely dried PNIPAM samples were prepared to cylinder type, with 7 mm in diameter and 13 mm in height. Due to the geometric testing error, the mass of the series dried PNIPAM ranges from 0.4688 g to 0.4780 g. By placing each dry PNIPAM separately into a glass sample bottle, DI water was added to the surface of PNIPAM till adsorbing the water to the required water content. By placing each sealed bottle into the sample chamber, the LF-NMR testing was carried out, under room temperature.

Dynamic desorption process was also conducted by heating the sample with water content of 2.5 g/g to above the LCST and continuous heating for several minutes. After the one-by-one testing of the samples of different water content, the PNIPAM hydrogel of 2.5 g/g water content was placed into a water bath of 60°C. When the PNIPAM hydrogel become opaque, continue heated for 1 min. Then, wipe the bottle and put into the sample chamber for testing. After about 30 s testing, put the bottle back to the water bath for further heating. Repeat the steps, and the heating time are controlled at 1 min, 6 min and 8 min.

For the aforementioned testing process, T_2 transversal relaxation curves were measured by Carr–Purcell–Meiboom–Gill (CPMG) sequence. The number of echoes (NECH) was 400, with a scan number of 32. The other NMR parameters include SW=100 kHz, RG1 = 20.0 dB, RFD = 0.25 ms. The raw CPMG decay curves were fitted by continuous multi-exponential data via the simultaneous iterative reconstruction technique (SIRT) algorithm.

Desorption in closed environment

The most commonly adopted method for testing the absorption/desorption rate is the consecutive method, by placing an electronic balance into the constant temperature and humidity box.[17] By using the consecutive testing methods, only total desorption amount can be obtained. As the experiment target of the current research is to clarify the desorption ratio of liquid water and water vapor, consecutive testing was not applicable. Thus, quasi static method that using desorption amount under several specific time points to generate the desorption rate curve was adopted. Both constant temperature and humidity box and constant temperature oven were adopted for the desorption performance of the closed environment experiment.

Before the desorption experiment of PNIPAM hydrogel, the evaporation rate and evaporation amount were quantified by testing only liquid water, for temperature variating from 40°C to 60°C. The DI water was injected into the empty container until approximately half of its volume. The diameter of the box is 80 mm and the height is 55 mm, in order to facilitate the removal of PNIPAM hydrogel after heating process. Then, the container was put into the constant temperature oven for more than 1 h, ensuring the temperature constant of water can container. The container was weighted, and then the cap of the container was tightened and sealed. The container was put back into the constant temperature oven for several minutes (5, 10, 20, 40 and 60 min, respectively). Then, the container was weighted again. The mass difference between the two weighing is the evaporation capacity. The maximum evaporation amount of 40°C, 50°C and 60°C are 0.0294 g, 0.0564 g and 0.1014 g, respectively, representing the equilibrium vapor and liquid phase. The water evaporation rate per unit area can be calculated when the exposed surface area of the water (equals to the bottom area of the container) was tested.

The completely dried PNIPAM hydrogel (about 1 g) was rehydrated to water content of 2.5 g/g with DI water. The initial size of the hydrated PNIPAM gel is 25 mm in length, 25 mm in width and 5 mm in thickness. The experiment procedure is shown in (Figure S2). Before the experiment, the PNIPAM hydrogel and the container was placed in the constant temperature and humidity box to unify the initial temperature and humidity. The temperature and relative humidity were controlled at 25°C, 60%. The setting temperature of the constant temperature oven was the designed desorption temperature of 40°C, 50°C and 60°C. The container containing the PNIPAM hydrogel was put into the constant temperature oven to begin the desorption process, and the timing was stated, simultaneously. When the surface of the PNIPAM hydrogel transformed from transparent to opaque states, the time was recorded. For the following experiment, the desorption time is controlled at extra 1, 3, 5, 10, 20 and 40 min, on the basis of the transparent to opaque states transformation time. When the timing was done for each desorption time, the container containing the PNIPAM hydrogel was taken out from the constant temperature oven, and the PNIPAM hydrogel was wiped by a weighted filter paper. Then, the mass of the PNIPAM hydrogel, the wet filter paper and the container were weighted, respectively. It should be noted that the wiping process can be done only after the transformation of PNIPAM hydrogel, as the opaque PNIPAM hydrogel gets not sticky when heated to above the LCST. All experiments in this session are based on the same PNIPAM sample, and the water adsorption/desorption cycle of the sample was done for more than 63 times. The desorption amount of liquid water and water vapor can be calculated by using the following (Equations 3, 4, and 5).

$$M_{liquid} = M_{l,contain} + M_{l,paper} + M_{l,evap} \quad \text{(Equation 3)}$$

$$M_{vapor} = M_{PNIPAM} - M_{liquid} - M_{l,evap} \quad \text{(Equation 4)}$$

$$M_{l,evap} = M_{evap}\frac{S_{PNIPAM}}{S_{base,contain}} \quad \text{(Equation 5)}$$

where M_{liquid} represents the liquid water desorption amount, M_{vapor} is the water vapor desorption amount, $M_{l,container}$ is the desorbed liquid water remaining in the container after the heating process, $M_{l,paper}$ is the desorbed liquid water on the PNIPAM surface after the heating process, $M_{l,evap}$ is the evaporated liquid water from the surface of the PNIPAM after transformed to opaque, S_{PNIPAM} is the surface area of the PNIPAM hydrogel and $S_{base,contain}$ is the bottom area of the container.

Desorption in air convection environment

Forced convection with hot air can effectively improve the heat and mass transfer process. To research the desorption amount and liquid water desorption rate, a forced convection desorption experimental platform was designed and established. The PNIPAM hydrogel was prepared, with water content of 2.5 g/g, as thin plate. The initial length, width and thickness of the plate PNIPAM is 70 mm, 70 mm and 5 mm, respectively. The schematic figure and the photograph of the experimental setup are shown in (Figures S3A and S3B).

A temperature and humidity chamber were utilized for controlling the temperature and humidity of the hot air. An evaporator for cooling and dehumidification, an electric heater for heating and a humidifier for humidification were incorporated in the chamber. a variable frequency fan mounted at the end of the hot air duct was used for extracting the hot air from the temperature and humidity chamber. A nozzle box on the hot air duct was used for testing the air flowrate, by testing the static pressure difference before and after the nozzle with micromanometer. Two temperature and humidity sensors were installed at the upstream and downstream of the PNIPAM hydrogel test section, for testing the inlet and outlet air temperature and humidity variation affected by the water desorption process, respectively. Proportional-integral-derivative (PID) control was utilized for the operation of the evaporator, heater and humidifier according to the upstream temperature and humidity of the PNIPAM hydrogel test section. The detailed experimental setup and the testing devices are listed in (Table S1).

Before the desorption process begin, the temperature and humidity were set at the desired desorption air flow condition, and the air extracting fan was turned on. The frequency of the air extracting fan was adjusted to control the air flowrate at the required value. When the temperature and humidity at the upstream of the PNIPAM hydrogel test section were stably controlled at the set value, the prepared PNIPAM hydrogel test section was inserted into the experimental setup. Then, the PNIPAM hydrogel desorption experimental process under air convection is similar to the desorption experiment process of the static closed environment. All experiments in this session are based on the same PNIPAM sample, and the water adsorption/desorption cycle of the sample was done for more than 54 times.

QUANTIFICATION AND STATISTICAL ANALYSIS

The number of characterization experiment repeat of PNIPAM, including surface morphology, crystallinity, gel fraction, CME and thermal properties, is one times for each sample. For desorption experiment for PNIPAM, the LF-NMR tests were repeated for one time for each sample. Desorption experiment in both closed environment and air convection environment were repeated for three times for each time point, and the average value, maximum value and minimum value were calculated, using MS Excel.